ACADEMIC PRESS

Available online at www.sciencedirect.com

SCIENCE DIRECT®

Fungal Genetics and Biology 38 (2003) 237–249

FUNGAL GENETICS AND BIOLOGY

www.elsevier.com/locate/yfgbi

Co-expression of 15 contiguous genes delineates a fumonisin biosynthetic gene cluster in *Gibberella moniliformis*☆

Robert H. Proctor,* Daren W. Brown, Ronald D. Plattner, and Anne E. Desjardins

US Department of Agriculture, National Center for Agricultural Utilization Research, Agriculture Research Service, 1815 North University St., Peoria, IL 61604, USA

Received 18 April 2002; accepted 25 July 2002

Abstract

Fumonisins are mycotoxins produced by the maize pathogen *Gibberella moniliformis* and are associated with cancer in rodents. In this study, we determined the nucleotide sequence of a 75-kb region of *G. moniliformis* DNA and identified 18 heretofore undescribed genes flanking a cluster of five previously identified fumonisin biosynthetic (*FUM*) genes. Ten of the newly identified genes downstream of the cluster were coregulated with *FUM* genes and exhibited patterns of expression that were correlated with fumonisin production. BLASTX analyses indicated that the predicted functions of proteins encoded by the 10 genes were consistent with activities expected for fumonisin biosynthesis or self-protection. These data indicate that the 10 newly identified genes and the previously identified *FUM* genes constitute a fumonisin biosynthetic gene cluster. Disruption of two of the new genes, encoding longevity assurance factors, had no apparent effect on fumonisin production, but disruption of a third, encoding an ABC transporter, had a subtle effect on ratios of fumonisins produced.
Published by Elsevier Science (USA).

Keywords: *Gibberella moniliformis*; *Fusarium verticillioides*; Maize; Fumonisins; Mycotoxin biosynthesis; Gene cluster

1. Introduction

Fumonisins are mycotoxins produced by the maize pathogen *Gibberella moniliformis* Wineland (syn. *G. fujikuroi* mating population A; anamorph *Fusarium verticillioides* (Sacc.) Nirenberg, syn. *F. moniliforme* Sheldon) and several related species. These mycotoxins are structurally similar to the sphingolipid intermediates sphinganine and sphingosine, and they disrupt sphingolipid metabolism by inhibiting the enzyme ceramide synthase (sphinganine *N*-acyltransferase) (Wang et al., 1991). Fumonisins are associated with several animal diseases, including kidney and liver cancers in laboratory rodents (Howard et al., 2001), and the consumption of fumonisin-contaminated maize has been epidemiologically associated with human esophageal cancer in some regions of the world where maize is a dietary staple (Marasas, 2001). A causal relationship between sphingolipid disruption and fumonisin-associated diseases has not been established but it seems likely, given the roles of sphingolipids in cellular metabolism and differentiation.

Gibberella moniliformis is one of the most prevalent causes of ear, stalk, and seedling rots of maize, and frequently colonizes maize tissues without causing disease symptoms (Munkvold and Desjardins, 1997). The widespread association of maize and *G. moniliformis* results in frequent contamination of maize kernels with fumonisins. B-series fumonisins (FB_1, FB_2, FB_3, and FB_4), which are generally the most abundant fumonisins in naturally contaminated maize (Nelson et al., 1993), consist of a linear 20-carbon backbone, which has a polyketide origin, substituted at various positions with an amine, one to three hydroxyl, two methyl, and two tricarboxylic acid groups (Fig. 1). Precursor feeding studies have revealed the origins of some of these functional groups but have provided only limited in-

☆ *Disclaimer:* Names are necessary to report factually on available data; however, the USDA neither guarantees nor warrants the standard of the products, and the use of the name by USDA implies no approval of the product to the exclusion of others that may also be suitable.

* Corresponding author. Fax: 1-309-681-6686.
E-mail address: proctorh@ncaur.usda.gov (R.H. Proctor).

1087-1845/02/$ - see front matter. Published by Elsevier Science (USA).
doi:10.1016/S1087-1845(02)00525-X

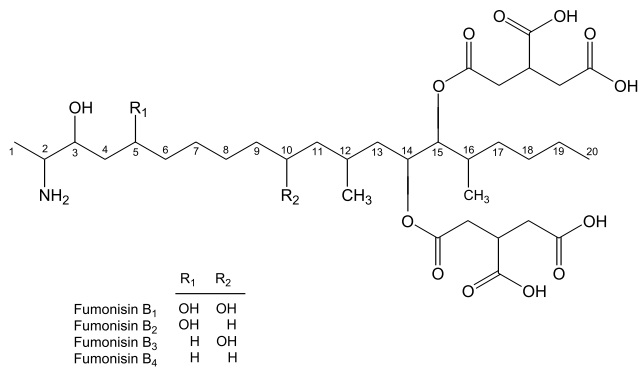

Fig. 1. Structures of B-series fumonisins.

formation on the order in which the groups are attached to the polyketide (Blackwell et al., 1994; Branham and Plattner, 1993; Caldas et al., 1998; Plattner and Shackelford, 1992; Proctor et al., 1999a,b).

In filamentous ascomycetes, genes involved in the biosynthesis of mycotoxins (e.g., aflatoxins, paxilline, and trichothecenes) and other secondary metabolites (e.g., gibberellins, lovastatin, and β-lactam antibiotics) are frequently organized into gene clusters (Brown et al., 2001; Keller and Hohn, 1997; Kennedy et al., 1999; Laich et al., 1999; Tudzynski and Holter, 1998; Young et al., 2001). The clustering of fumonisin biosynthetic genes was first evident from the tight linkage of three genetically defined *G. moniliformis* loci (*Fum1*, *Fum2*, and *Fum3*), variant alleles of which conferred altered fumonisin production phenotypes (Desjardins et al., 1996). Subsequently, five clustered genes (*FUM5*, *FUM6*, *FUM7*, *FUM8*, and *FUM9*) were identified, characterized, and shown via disruption and/or expression analyses to be involved in fumonisin biosynthesis (Proctor et al., 1999b; Seo et al., 2001). A recent complementation analysis also revealed that the *Fum1* locus and *FUM5* are the same gene, now designated *FUM1* (Proctor, Desjardins, and Plattner, unpublished). Another recently identified *G. moniliformis* gene, *FCC1*, plays a role in a signal transduction pathway that regulates fumonisin biosynthesis; however, there is no evidence to suggest that *FCC1* is clustered with the *FUM* genes (Shim and Woloshuk, 2001).

The further characterization of fumonisin biosynthetic genes will aid in elucidating the biochemical and regulatory pathways that culminate in the formation of these mycotoxins. In the current study, nucleotide sequence analyses of genomic DNA flanking previously characterized *FUM* genes revealed the presence of 18 additional genes. Expression analyses indicate that the 10 genes immediately downstream of *FUM9*, along with *FUM1*, *FUM6*, *FUM7*, *FUM8*, and *FUM9*, constitute a gene cluster that encodes most of the enzymatic activities predicted to be necessary for fumonisin biosynthesis.

2. Materials and methods

2.1. Strains and media

Strain M-3125 was the wild-type *G. moniliformis* strain used throughout this study (Leslie et al., 1992). For DNA isolation, the fungus was grown in liquid GYEP medium (2% glucose, 1% peptone, and 0.3% yeast extract) (Desjardins et al., 1996). Cosmid clones Cos16-1, Cos6B, and Cos4-5 were isolated from a genomic library prepared from *G. moniliformis* strain M-3125, as previously described (Proctor et al., 1999b; Seo et al., 2001).

2.2. Fumonisin analysis

Fumonisin production in *G. moniliformis* strains was determined from cracked maize and liquid GYAM (0.24 M glucose, 0.05% yeast extract, 8 mM L-asparagine, 5 mM malic acid, 1.7 mM NaCl, 4.4 mM K_2HPO_4, 2 mM $MgSO_4$, and 8.8 mM $CaCl_2$, pH 3.0) cultures that were prepared, as previously described (Seo et al., 2001). Production by all strains was determined via HPLC analysis with orthophthalaldehyde-derivatized samples (Sydenham et al., 1992). Production by selected strains was also determined via liquid chromatography-mass spectrometry (LC-MS), as previously described (Plattner et al., 1996).

2.3. Nucleic acid manipulations and sequence analysis

The nucleotide sequence of cosmid clone Cos4-5 was determined with the Genome Priming System (GPS) (New England BioLabs, Beverly, MA) and primer walking. The nucleotide sequences of portions of Cos16-1 and Cos6B were determined from fragments subcloned into pBluescriptII (Stratagene, La Jolla, CA) with vector-specific primers and primer walking. All sequencing reactions were carried out with BigDye Cycle Sequencing Kit reagents (Perkin–Elmer Applied Biosystems, Foster City, CA) following manufacturer's instructions. Sequencing templates were generated via an alkaline lysis minipreparation procedure for cosmid clones (Sambrook et al., 1989) and via the UltraClean Mini Plasmid Prep Kit (MoBio Laboratories, Solana Beach, CA) for subclones in pBluescript. Nucleotide sequence reactions were analyzed on an ABI Prism 377 DNA Sequencer (Perkin–Elmer Applied Biosystems, Foster City, CA). Sequence information was assembled and edited using the Sequencher program (Gene Codes, Ann Arbor, MI). Nucleotide sequence comparisons were done with the BLASTX program employing the nonredundant database of the National Center for Biotechnology Information (NCBI-NR) (Altschul et al., 1997).

For PCR analysis, *G. moniliformis* genomic DNA was isolated with the UltraClean DNA Purification Kit

(MoBio Laboratories, Solana Beach, CA). Approximately 50 mg lyophilized mycelium was ground to a powder, mixed with extraction buffer (200 mM Tris, pH 8.5; 250 mM NaCl; 25 mM EDTA, pH 8.0, and 0.5% SDS), extracted with 1:1 (v/v) phenol:chloroform, and centrifuged for 10 min. The aqueous phase was then subjected to the UltraClean protocol by mixing it first with a sodium iodide solution, then with UltraBind beads, and finally recovering DNA from the beads with water as specified by the manufacturer. For Southern blot analyses, genomic DNA was isolated from approximately 50 mg lyophilized mycelium via the DNeasy protocol (Qiagen, Valencia, CA).

Total RNA was isolated from *G. moniliformis* via the TRIzol method (Gibco BRL, Gaithersburg, MD) and Northern blots were carried out, as previously described (Seo et al., 2001). DNA probes for Southern and Northern blot hybridization were labeled with [^{32}P]dCTP with the Prime-A-Gene system (Promega, Madison, WI). DNA templates used to synthesize hybridization probes consisted of 700–1200-bp fragments of coding regions amplified by PCR from cosmid clones or plasmids with *G. moniliformis* DNA-specific primers.

2.4. Gene disruption and transformation

The disruption of *FUM17*, *FUM18*, and *FUM19* was done via the protoplast method with hygromycin B resistance as the selectable marker (Proctor et al., 1999b; Seo et al., 2001). *FUM17* and *FUM18*, which lie adjacent to one another and in opposite orientations (Fig. 2), were disrupted simultaneously with disruption vector pFUM17/18::HYG. This vector consisted of a DNA fragment spanning *FUM17* and *FUM18* from which an internal fragment, including > 75% of both coding regions, was removed and replaced with the hygromycin B resistance gene *HygB* (Turgeon et al., 1987). The vector was constructed by first amplifying DNA fragments UF17 and UF18 by PCR. Fragment UF17 spanned from 1240 bp upstream to 302 bp downstream of the *FUM17* start codon and was amplified with primers rp334 (5′-GCTAAGCTTCCATCAGTTACAGAACCATGTC-3′) and rp335 (5′-GCTACTAGTGATGCAGCAACCGTTTGGAAG-3′). Fragment UF18 spanned from 1204 bp upstream to 318 bp downstream of the *FUM18* start codon and was amplified with primers rp332 (5′-CGAGGTACCGATGCAAGGTCAAGGTTGTAC-3′) and rp333 (5′-CGACTCGAGACGTATAGGGTTCTGCTTGAG-3′). The underlined bases in the primer sequences above are restriction sites that were incorporated into the primers. Fragments UF17 and UF18 were cloned into PCR cloning vector pT7Blue-3 (Novagen, Madison, WI) and UF18 was then cloned, via the *Kpn*I and *Xho*I sites incorporated into the PCR primers, upstream of *HygB* in pUCH2-8 to yield vector pUF18/HYG. Fragment UF17 was removed from pT7Blue via *Nhe*I/*Sna*BI digestion and placed downstream of *HygB* in pUF18/HYG cut with *Spe*I and *Sma*I to yield pFUM17/18::HYG.

FUM19 was disrupted independently with disruption vector pFUM19::HYG, which was constructed by first excising from Cos4-5 a 5300-bp *Eco* RI fragment. This fragment spanned from 150 bp upstream of the *FUM19* start codon to 353 bp downstream of the *FUM19* stop codon. An internal 1713-bp *Sal*I fragment, which corresponded to nucleotides 2014–3726 of the *FUM19* coding region, was excised from the *Eco*RI fragment and replaced with *HygB*.

Hygromycin B-resistant, putative transformants were isolated from a single conidium, prior to DNA and fumonisin analyses. Colonies derived from a single conidium were screened by PCR to determine whether disruption vectors integrated at the target site via homologous recombination. This initial PCR screen employed *HygB*-specific primers 1098 (5′-ACCAAGCCTATGCCTACAGCATCC-3′) and rp250 (5′-CTGCTGCATTCCCATTCCCATCGT-3′) in combination with *Fusarium*-specific primers rp403 (GATCCTAGGCAACACAGGCAAGAG) and rp404 (5′-AAGCCTCTACTTACTGCCTGCAAG-3′) for *FUM17*/*FUM18* disruption and rp402 (5′-CGTGTTAGGGTAAGGGCAGTTAAC-3′) and rp412 (5′-ACTCTGGGAAGCTACTTCATACCT-3′) for *FUM19* disruption. The *Fusarium*-specific

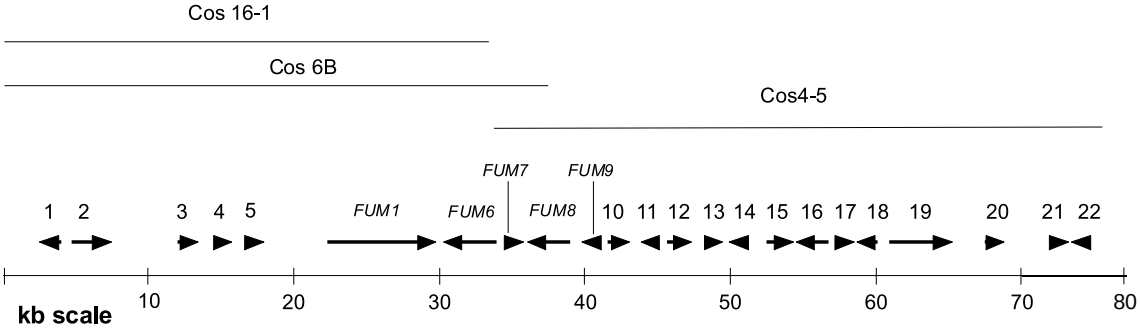

Fig. 2. Map of cosmid clones Cos16-1, Cos6B, and Cos4-5 showing positions of newly identified ORFs and previously identified genes *FUM1* and *FUM6–FUM9*. Arrows indicate locations and orientations of genes. The nucleotide sequence represented here has been included in GeneBank as an update to Accession AF155773.

primers were complementary to DNA flanking the DNA sequences used to construct the disruption vectors. Homologous and ectopic integration of vector DNA in transformants was confirmed by Southern blot analysis. A subset of transformants was then analyzed by HPLC and LC-MS for their ability to produce fumonisins.

3. Results

3.1. Identification of open reading frames

We determined the nucleotide sequence of three overlapping cosmid clones that included the previously described *FUM1* (=*FUM5*), *FUM6*, *FUM7*, *FUM8*, and *FUM9* genes (Proctor et al., 1999b; Seo et al., 2001) as well as flanking DNA. The sequence has been included in the GenBank database as an update to Accession No. AF155773. The sequenced region spans approximately 75 kb and includes 18 putative open reading frames (ORFs) in addition to the five previously described genes (Fig. 2). For the purposes of this study, all ORFs to the left of *FUM1* in Fig. 2 are considered to be upstream of *FUM1* and all genes to the right of *FUM9* in Fig. 2 are considered to be downstream of *FUM9*. Five of the ORFs (ORF1–ORF5) are located upstream of *FUM1*, while the remaining 13 ORFs (ORF10–ORF22) are located downstream of *FUM9*. In the region between *FUM1* and ORF19, there are no DNA sequences over 1210 bp that do not include ORFs with similarity to previously described sequences. Within this region, the start and/or stop codons of adjacent ORFs are 113–705 bp apart when adjacent coding regions are oriented in a 3′-to-3′ manner and 446–1208 bp when coding regions are oriented in a 3′-to-5′ or 5′-to-5′ manner. In other regions of the 75 kb of sequenced DNA, there are considerably longer stretches between ORFs; 4.4 kb between ORF5 and *FUM1*, 4.5 kb between ORF2 and ORF3, 2.3 kb between ORF19 and ORF20, and 3.1 kb between ORF20 and ORF21.

BLASTX analyses revealed that the predicted proteins corresponding to ORFs 1–5, 10–19, and 22 share significant similarity ($E < 0.05$) to protein sequences in the NCBI-NR database (Table 1). Of the five ORFs upstream of *FUM1*, two appear to encode regulatory proteins: the predicted ORF2 protein is similar to several regulatory proteins with tryptophan-aspartic acid repeats, and the ORF4 protein included a region that is similar to the cysteine-rich zinc finger domains of some transcription factors and kinases (Table 1). RPS-BLAST analysis of ORF4 did not reveal similarities to any protein families in the NCBI Conserved Domain Database. The other three ORFs upstream of *FUM1* appear to encode metabolic enzymes. The predicted ORF1 protein is highly similar to the NAD metabolic enzyme nicotinate phosphoribosyltransferase, the predicted ORF3 protein is similar to the protein deglycosylation enzyme peptide *N*-glycanase, and the ORF5 protein is similar to enzymes with carbonyl reductase activities (Table 1). RPS-BLAST analysis of ORF5 revealed that it was similar to pfam00104 (score 61.8 bits, *E* value 2×10^{-11}), a family of zinc-binding dehydrogenases.

BLASTX analyses also indicated that most of the ORFs downstream of *FUM9* encode metabolic enzymes or transporters (Table 1). The exceptions to this are the predicted ORF 20 and 21 proteins, which both have insignificant levels of similarity (BLAST *E* values > 0.1) to zinc finger domains of transcription factors and/or kinases. The predicted ORF10 and ORF16 proteins share significant similarity to fatty acyl-coenzyme A (CoA) synthetases, enzymes that esterify CoA to fatty acids and other acyl compounds during transport across plasma membranes or prior to reactions with other organic molecules. The ORF11 protein is most similar to a group of tricarboxylate transporters located in the inner mitochondrial membrane. The predicted ORF12 and ORF15 proteins are highly similar to cytochrome P450 monooxygenases. The ORF13 protein is similar to cinnamoyl CoA reductases and dihydroflavonol reductases, which are carbonyl reductases. RBS-BLAST analysis indicated that ORF13 shares similarity with pfam01073 (score 43 bits, *E* value 2×10^{-5}), the 3-β hydroxysteroid dehydrogenase/isomerase protein family. These proteins are part of the superfamily of proteins known as short-chain dehydrogenases/reductases (SDR), which includes cinnamoyl CoA and dihydroflavonol reductases. SDRs can have as little as 10% amino acid sequence identity, but share two short conserved regions, the N-terminal coenzyme-binding motif, $TGX_{2-3}GX_{1-2}G$, and the active site motif, YX_3K (Jörnvall et al., 1995; Lacombe et al., 1997). Both motifs are present in the predicted ORF13 protein (Fig. 3). BLASTX and RPS-BLAST analyses of the predicted ORF14 protein revealed that it is similar to the condensation domains of multifunctional peptide synthetases (Table 1). The ORF14 protein exhibits low levels of sequence similarity and identity to these proteins along its entire length and has a DHTHCDA motif, which is similar to HHXXXDG, the proposed active site motif of condensation domains (Fig. 3) (Stachelhaus et al., 1998). These domains catalyze amide bond formation during synthesis of peptides via a mechanism that does not directly involve ribosomes (Marahiel et al., 1997).

The predicted ORF17 and ORF18 proteins are similar to longevity assurance (LA) factors, which are likely to be components of CoA-dependent ceramide synthase (Table 1) (Guillas et al., 2001; Schorling et al., 2001). Interestingly, an LA-like gene, *Asc-1*, in tomato confers resistance to fumonisin B_1 and to the structurally related

Table 1
Description of genes identified on cosmid clones Cos16-1, Cos6B, and Cos4-5

ORF[a]	Name[b]	Putative function[c]	BLAST *E* value[d]	Coding region[e] (bp)	Amino acids[f]	Intron lengths[g] (bp)	Accession No.
1	*NPT1*	Nicotinate phosphoribosyl transferase	10^{-98}	1492	459	50, 62	NP_594094
2	*WDR1*	WD protein	10^{-78}	2689	856	48, 70	NP_596540
3	*PNG1*	Peptide *N*-glycanase	10^{-81}	1409	450	55	NP_015229
4	*ZNF1*	Transcription factor/kinase	10^{-8}	975	325	None	BAB24549
5	*ZBD1*	Zinc-binding dehydrogenase/reductase	10^{-10}	854	259	77	AAL06644
	FUM1	Polyketide synthase	0.0	8163	2607	57, 65, 70, 62, 85	ADD34559
	FUM6	Cytochrome P450 Monooxygenase	0.0	3593	1115	61, 130, 54	BAA82526
	FUM7	Dehydrogenase	10^{-21}	1275	424	None	NP_343836
	FUM8	Aminotransferase	10^{-29}	2532	839	80, 127, 86, 122	O54649
	FUM9	Dioxygenase	10^{-57}	903	300	None	AAK01519
10	*FUM10*	Fatty acyl-CoA synthetase	10^{-68}	1482	493	None	NP_588549
11	*FUM11*	Tricarboxylate transporter	10^{-59}	1164	295	156, 58, 62	NP_594420
12	*FUM12*	Cytochrome P450 Monooxygenase	10^{-75}	1735	511	42, 93, 62	Q00707
13	*FUM13*	Short-chain dehydrogenase/reductase	10^{-13}	1110	369	None	NP_593981, T02760
14	*FUM14*	Peptide synthetase condensation domain	10^{-11}	1320	439	None	CAA61605
15	*FUM15*	Cytochrome P450 monooxygenase	10^{-30}	1856	576	60, 65	NP_354568
16	*FUM16*	Fatty acyl-CoA synthetase	0.0	2223	683	79, 47, 45	T49727
17	*FUM17*	Longevity Assurance Factor	10^{-66}	1236	388	69	NP_596102
18	*FUM18*	Longevity assurance factor	10^{-46}	1524	427	120, 61, 59	NP_593201
19	*FUM19*	ABC Transporter	10^{-106}	4806	1489	121, 57, 59, 99	CAC28822
20	ORF20	Transcription factor	0.18	1323	440	None	
21	ORF21	Transcription factor/kinase	1.8	822	273	None	
22	*MPU1*	Mannose-P-Dolichol Utilization	10^{-33}	919	288	52	BAB64924, Q9VMW8

[a] ORF numbers are the same as shown in Fig. 1.
[b] *FUM1* and *FUM6–FUM9* were described previously (Proctor et al., 1999b; Seo et al., 2001) and are included here for the sake of completion.
[c] Determination of putative functions was based on the highest BLASTX scores. The functions listed are the same as the proteins that yielded the highest BLASTX score for each ORF.
[d] Highest *E* value from BLASTX analysis of each ORF with putative introns removed from sequence.
[e] Length of coding region including putative introns.
[f] Number of amino acids encoded by each ORF.
[g] Lengths of putative introns within each ORF. None indicates that no introns were predicted within the ORF. Introns were predicted based on consensus sequences for 5′ and 3′ splice and internal motifs for filamentous fungi (Gurr et al., 1987) and from introns identified previously in *FUM1*, *FUM6*, and *FUM8* via sequence analysis of cDNAs (Proctor et al., 1999b; Seo et al., 2001).

AAL-toxin, which is produced by the tomato pathogen *Alternaria alternata* f. sp. *lycopersici* (Brandwagt et al., 2000). The ORF19 protein is highly similar to ABC transporters, which are located in the cell membrane (Table 1). Finally, the ORF 22 protein was highly similar to a mannose-P-dolichol utilization protein of *Magnaporthe grisea* and several animal species.

3.2. Intron analysis

We predicted the presence of 26 introns within the 18 newly identified ORFs. The putative introns were identified based on the presence of sequences similar to 5′ and 3′ splice and internal motifs for fungal introns and the fact that removal of the putative introns from the coding sequence corrected reading frame shifts in the ORFs. These introns along with the 12 previously identified in *FUM1*, *FUM6*, *FUM7*, *FUM8*, and *FUM9* vary in length from 42 to 156 bp with an average length of 75 bp. The consensus sequences for the 5′, internal, and 3′ intron motifs are GTRHGT, WDCTRAYH, and YAG, respectively, where R indicates A or G, Y indicates C or T, W indicates A or T, D indicates A, G or T, and H indicates A, C, or T. The consensus base or combination of bases shown for each position occurred in at least 75% of the introns (Fig. 4). The first G in the 5′ motif and the CT in the internal motif are invariable while the first T in the 5′ motif occurs in 94% of the introns and the AG in the 3′ motif occurs in 97% of the introns. The intron consensus sequences described above are consistent with the 5′, internal, and 3′ motifs reported in eight previously described introns found in the *G. moniliformis FCC1* and *MAT* genes (Shim and Woloshuk, 2001; Yun et al., 2000). The *G. moniliformis* intron consensus sequences are also similar to those described for introns in the trichothecene biosynthetic gene clusters in *F. graminearum* and *F. sporotrichioides* (Brown et al., 2001). However, *G. moniliformis* introns tend to exhibit more sequence variations, particularly at the second and fifth positions of the 5′ splice sequence.

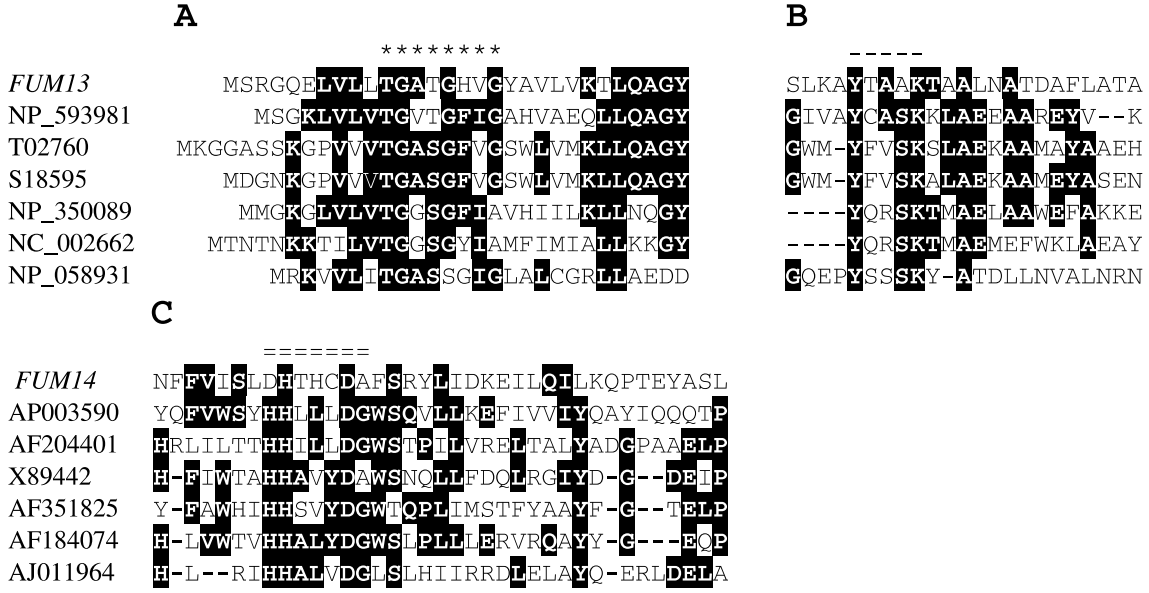

Fig. 3. (A) Alignment of residues 1–30 of the predicted ORF13 (= *FUM13*) protein with six short-chain dehydrogenases/reductases (SDRs). The putative coenzyme-binding motif is indicated by ☆☆☆☆☆☆☆☆. (B) Alignment of residues 172–194 of the ORF13 protein with the same six SDRs. The putative active site motif is indicated by −−−−−. (C) Alignment of residues 128–157 of the predicted ORF14 (= *FUM14*) protein with condensation domains from six peptide synthetases. The putative active site is indicated by = = = = = = = =. The order of amino acid sequences is the same in (A) and (B). Accession Nos., (A) and (B) NP_593981, *Schizosaccharomyces pombe* cinnamoyl-CoA reductase; T02760, Zea mays dihydroflavonol-4-reductase; S18595, *Hordeum vulgare* dihydroflavonol-4-reductase; NP_350089, *Clostridium acetobutylicum* nucleoside–diphosphate–sugar epimerase; NC_002662, *Lactococcus lactis* subsp. *lactis* oxidoreductase; NP_058931, *Rattus norvegicus* hydroxysteroid 17-β dehydrogenase; (C) AP003590, *Nostoc* sp. PCC 7120 microcystin synthetase B; AF204401, *Streptomyces chrysomallus* actinomycin synthetase III; X89442, *Metarhizium anisopliae* peptide synthetase condensation domain 1; AF351825, *Hypocrea virens* peptide synthetase; AF184074, *Alternaria alternata* AM-toxin synthetase; AJ011964, *Claviceps purpurea* D-lysergyl-peptide-synthetase. Sequence alignments were done with the Genetics Computer Group PileUp and DNAMAN protein alignment programs.

3.3. Expression of ORFs

To determine whether any of the 18 newly identified ORFs are associated with fumonisin biosynthesis, we analyzed their expression in GYAM medium, which is conducive to fumonisin production. Previous analyses showed that the expression of *FUM1*, *FUM6*, *FUM7*, *FUM8*, and *FUM9* is highly correlated with fumonisin production (Seo et al., 2001; Shim and Woloshuk, 2001). For Northern blot analyses, we used total RNA isolated from liquid GYAM cultures of *G. moniliformis* before and after the onset of fumonisin production (Proctor et al., 1999a,b). ORFs 10–19 exhibited patterns of expression that were similar to those of *FUM7* and *FUM9* (Fig. 5)

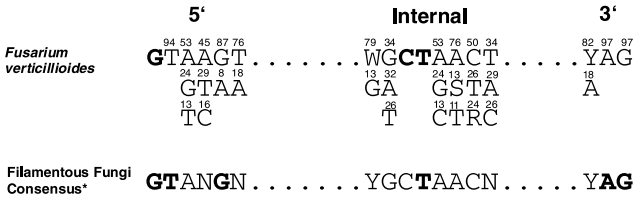

Fig. 4. 5′, Internal, and 3′ sequence motifs for 27 predicted and 12 confirmed introns in the *G. moniliformis* genes and ORFs shown in Fig. 1. Numbers indicate the frequencies of occurrence of the bases immediately below them in all 39 introns.

and to the previously described patterns of *FUM6* and *FUM8* (Seo et al., 2001). That is, no transcript was visible at 52 or 64 h after inoculation, low levels of transcript were visible at 76 h, and high levels of transcripts were visible at 88 and 100 h. This pattern of expression was correlated with fumonisin production in the same cultures: fumonisin B_1 was not detected at 52 and 64 h but was detected at increasing levels at 76 (0.6 μg/ml), 88 (2.2 μg/ml), and 100 (8 μg/ml) h after inoculation (Seo et al., 2001). In contrast, transcripts of ORFs 1, 2, 5, 21, and 22 were visible at all time points examined (Fig. 5) and transcripts of ORFs 3, 4, and 20 were not visible at any of the time points examined (not shown).

Because ORFs 10–19 were coregulated with previously identified fumonisin biosynthetic genes and because their expression was correlated with fumonisin production in GYAM medium, we have given these ORFs *FUM* gene designations (Table 1).

3.4. Disruption of FUM17, FUM18, and FUM19

The disruption strategy for *FUM17* and *FUM18* was such that homologous recombination of the disruption vector pFUM17/18::HYG on both sides of *HygB* with the *G. moniliformis* genome would simultaneously disrupt *FUM17* and *FUM18* by replacing over 75% of the

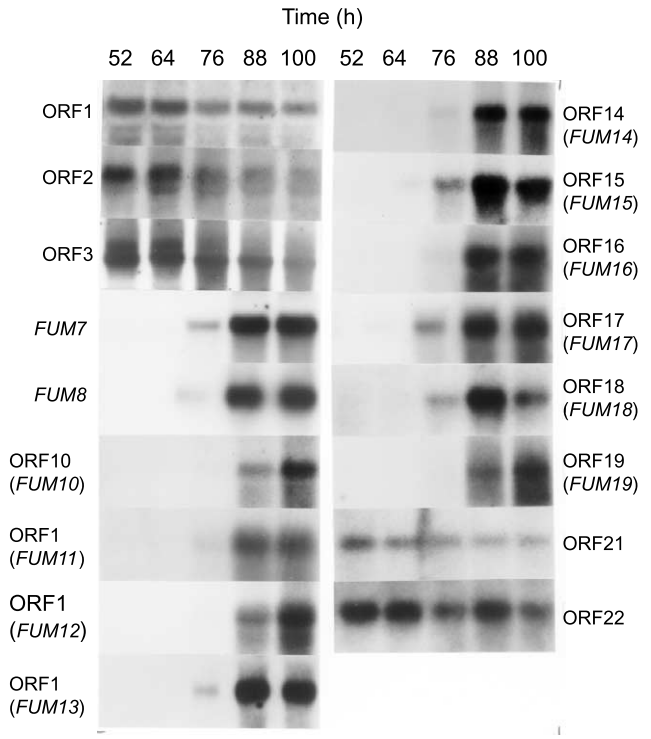

Fig. 5. Northern blot analysis of ORFs identified in this study. Total RNA was isolated from wild-type *G. moniliformis* strain M-3125 grown in liquid GYAM medium. ^{32}P-labeled hybridization probes were prepared from PCR products amplified from within each ORF examined. The fumonisin levels in the cultures from which total RNA was isolated were 0, 0, 0.6, 2.2, and 8 μg/ml at 52, 64, 76, 88, and 100 h, respectively (Proctor et al., 1999b). Expression data for ORFs 3, 4, and 20 are not presented because no transcripts were observed for these ORFs under the conditions of this experiment. As reported previously (Seo et al., 2001), the expression patterns for *FUM6*, *FUM7*, *FUM8*, and *FUM9* were very similar to one another. We have included the previously published data for *FUM7* and *FUM8* here for the purpose of comparison.

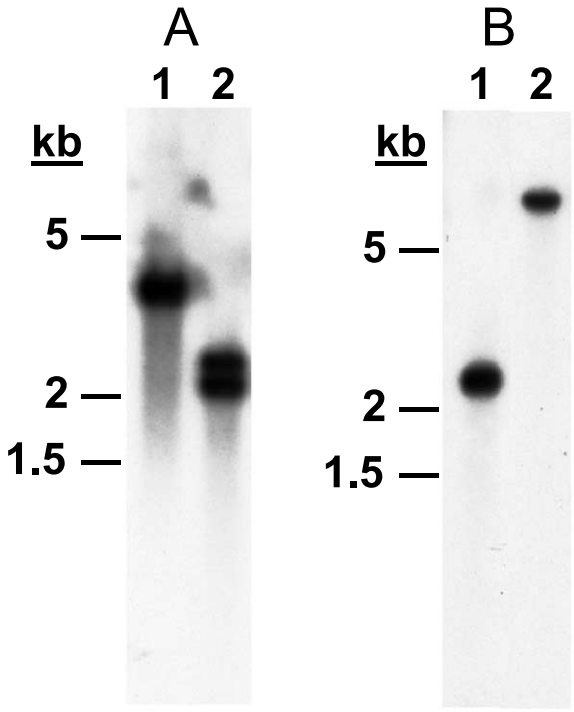

Fig. 6. Southern blot analyses of *FUM17*/*FUM18* (A) and *FUM19* (B) disruption mutants. For the *FUM17*/*FUM18* mutant, total genomic DNA was digested with restriction enzyme *Pst*I, electrophoresed, transferred to a nylon membrane, and then hybridized to a ^{32}P-labeled probe consisting of fragments UF17 and UF18 (see Materials and methods). This treatment should generate two hybridizing fragments of 3700 and 3823 bp for the wild-type progenitor strain (panel A, lane 1) and two smaller hybridizing fragments of 2597 and 2745 bp for *FUM17*/*FUM18* disruption mutants (panel A, lane 2). For *FUM19*, genomic DNA was digested with restriction enzyme *Stu*I, electrophoresed, transferred to a nylon membrane, and then hybridized to a [^{32}P]-labeled probe consisting of the 5300-bp fragment used to construct the *FUM19* disruption vector without the internal 1713-bp *Sal*I fragment (see Materials and methods). This treatment should yield two hybridizing fragments of 2431 and 2464 bp for the wild-type progenitor strain (panel B, lane1) and a single larger fragment of 5683 bp for *FUM19* disruption mutants (panel B, lane 2). Data for only one of each type of disruption mutant are presented.

coding regions of both genes and the 3′ flanking region between them with *HygB*. Sixty hygromycin B-resistant putative transformants were recovered following transformation of wild-type strain M-3125 with pFUM17/18::HYG. Results of PCR analyses were consistent with the disruption vector integrating via double homologous recombination events in 42%, via single homologous recombination events in 48%, and via nonhomologous integration events in 10% of the transformants. Southern blot analysis of genomic DNA of a subset of 10 transformants confirmed that *FUM17* and *FUM18* were disrupted in five transformants (Fig. 6). These five disruption mutants, as well as all other transformants examined, produced fumonisins B_1, B_2, and B_3 in GYAM and cracked maize medium at levels similar to the wild-type progenitor strain. For example, in GYAM medium *FUM17*/*FUM18* disruption mutants produced 219–259, 20–25, and 11–12 μg/ml FB_1, FB_2, and FB_3, respectively. Wild-type strain M-3125 produced 246, 31, and 26 μg/ml FB_1, FB_2, and FB_3, respectively, in GYAM.

The disruption strategy for *FUM19* was such that homologous recombination of disruption vector pFUM19::HYG on both sides of *HygB* with the *G. moniliformis* genome would replace a 1713-bp internal fragment of the *FUM19* coding region with *HygB* and therefore disrupt *FUM19*. Forty-six hygromycin B-resistant putative transformants were recovered following transformation of strain M-3125 with pFUM19::HYG. Single-conidium isolates of each putative transformant were analyzed via PCR to determine whether the disruption vector integrated via single or double homologous or nonhomologous recombination. Southern blot analysis of genomic DNA from a subset of 12 transformants confirmed that *FUM19* was disrupted in three transformants (Fig. 6). *FUM19* disruption mutants produced FB_1, FB_2, and FB_3 in both GYAM and

Table 2
Reduced percentage of FB_3 in GYAM cultures of *FUM19* disruption mutants GfA2637, GfA2646, and GfA2653 compared to their wild-type progenitor strain M-3125 and transformant GfA2636, which contains the *FUM19* disruption vector but has a wild-type *FUM19*

Strain No.	Genotype[a]	Percent total fumonisins[b]		
		FB_3	FB_1	FB_2
M-3125	WT *FUM19*	13	78	11
GfA2636	WT *FUM19*	10	81	9.4
GfA2637	Δ*FUM19*	1.8	90	8.2
GfA2646	Δ*FUM19*	1.6	90	8.4
GfA2653	Δ*FUM19*	1.5	90	8.7

[a] WT *FUM19* indicates wild-type *FUM19* and Δ*FUM19* indicates a disrupted *FUM19*.

[b] For each strain, percent total fumonisin was calculated by dividing the concentration of individual fumonisins by the combined concentration of FB_1, FB_2, and FB_3, and multiplying by 100. For Δ*FUM19* strains, the concentrations of FB_1, FB_2, and FB_3 ranged from 145–243, 13–24, and 3–4 μg/ml GYAM, respectively. For WT *FUM19* strains, the concentrations of FB_1, FB_2, and FB_3 ranged from 155–265, 18–31, and 27–33 μg/ml GYAM, respectively.

cracked maize media. However, in GYAM medium, the disruption mutants consistently produced lower levels of FB_3 than their wild-type progenitor strain M-3125 and transformants of M-3125 with a wild-type *FUM19* (Table 2). FB_3 constituted only 1.5–1.8% of the total fumonisin content ($FB_1 + FB_2 + FB_3$) in GYAM cultures of *FUM19* disruption mutants, but 10–13% of the total content in cultures of M-3125-derived strains with a wild-type *FUM19*. The marked reduced production of FB_3 by the mutants, relative to strains with a wild-type *FUM19*, did not occur in cracked maize cultures (not shown).

4. Discussion

In filamentous fungi, genes responsible for the biosynthesis of a given secondary metabolite tend to be coordinately regulated and located together in gene clusters. Previously, we reported a cluster of five fumonisin biosynthetic genes, *FUM1*, *FUM6*, *FUM7*, *FUM8*, and *FUM9* (Seo et al., 2001). The results of the current study indicate that the fumonisin biosynthetic gene cluster includes 10 additional genes located immediately downstream of *FUM9* (Fig. 2). This conclusion is based on the observation that the 10 newly identified genes are coregulated with the five previously identified *FUM* genes and that expression of all 15 genes in the cluster is correlated with fumonisin production. In contrast, genes in the same region but outside the putative cluster do not exhibit patterns of expression that are correlated with fumonisin production. The predicted functions of most of the 10 new *FUM* genes are consistent with activities expected to be required for fumonisin biosynthesis or self-protection. Interestingly, none of the 15 genes within the cluster appears to be a regulatory gene. Transcription factors and other regulatory genes have been identified in several other fungal secondary metabolite gene clusters (Hohn et al., 1999; Kennedy et al., 1999; Woloshuk et al., 1994; Young et al., 2001).

The effect of *FUM19* disruption on fumonisin biosynthesis was subtle. In liquid GYAM medium, disruption mutants produced fumonisins, but the ratio of FB_3 to the total fumonisin content ($FB_1 + FB_2 + FB_3$) was reduced. A possible explanation for this phenotype is that elimination of the *FUM19*-encoded transporter in the *FUM19* mutants reduces the efficiency of fumonisin export from hyphae and thereby results in fumonisins remaining in hyphae for longer periods of time. This in turn might allow for a greater percentage of FB_3 to be converted to FB_1. This hypothesis is consistent with previous studies that demonstrated that *G. moniliformis* readily converts FB_3 to FB_1 but does not convert FB_2 to FB_1 (Proctor et al., 1999a,b). The levels of FB_2 produced by the *FUM19* mutants were essentially the same as those produced by the wild type (Table 2).

Disruption of *FUM17* and *FUM18* did not noticeably alter fumonisin production and therefore demonstrated that these genes are not required for fumonisin biosynthesis. Despite these results, the two genes were included in the fumonisin gene cluster because of their location and their coregulation with other *FUM* genes. Even though *FUM19* mutants were reduced in the amount of FB_3 they produced, *FUM19* is similar to *FUM17* and *FUM18* in that it is not essential for fumonisin production. There are other examples of fungal genes that are located in secondary metabolite gene clusters but that are not required for production of the metabolite(s). The *Aspergillus nidulans* sterigmatocystin gene cluster, the *F. sporotrichioides* trichothecene gene cluster, and *F. fujikuroi* gibberellin gene cluster all include one or more genes that are coregulated with other genes in the clusters but that are not required for the production of the respective metabolites (Brown et al., 2002; Voss et al., 2001) (Keller, personal communications). The raison d'etre for such genes is not clear, but the fact that they are not required for production of the metabolites in question suggests that they may be indirectly involved in production and/or that their functions may be redundant.

Indirect roles in secondary metabolite biosynthesis include transport and self-protection. A self-protection function for *FUM17* and *FUM18* is consistent with their similarity to the tomato longevity assurance (LA) factor gene, *Asc-1*, that confers resistance to fumonisin B_1 and the structurally similar AAL-toxins (Brandwagt et al., 2000). Likewise, transport and self-protection functions for the *FUM19* protein are consistent with its similarity to ABC transporters, which act as efflux pumps that transport compounds from inside cells to the sur-

rounding environment. This efflux pump activity of some ABC transporters can reduce cellular concentrations of toxic molecules and thereby confer protection from them. Very little is known about the toxicity of fumonisins to *G. moniliformis*, and as a result, it is not known whether the fungus requires a self-protection mechanism against fumonisins. In one study, which compared the effect of fumonisin B_1 on the spore germination and mycelial growth of several fungal species, *G. moniliformis* was more tolerant of fumonisin B_1 than some species but not others (Keyser et al., 1999). A comparison of the effects of fumonisin on growth of and sphingolipid metabolism in *FUM17*/*FUM18* and *FUM19* disruption mutants relative to the wild type may help to elucidate whether these genes play a role in self-protection.

The possibility that *FUM17*, *FUM18*, and *FUM19* have redundant functions is plausible given the precedence for redundant genes in other fungi. This redundancy could result from gene duplication, such as in *Cochliobolus carbonum* where some HC-toxin biosynthetic genes can be present in two or more copies (Ahn et al., 2002). During our Southern blot analyses of *FUM17*/*FUM18* and *FUM19* disruption mutants, however, we found no evidence for duplication of these genes. Our standard Southern blot hybridization conditions are not able to detect genes that are less than $\sim 80\%$ identical to the hybridization probes. Therefore, if *FUM17*, *FUM18*, and/or *FUM19* were duplicated but the homologs were less than $\sim 80\%$ identical to them, we would not have detected the homologs in our Southern blot analyses.

Redundancy of function could also result from genes involved in other metabolic processes compensating for *FUM17*, *FUM18*, and *FUM19* in the disruption mutants. In *Saccharomyces cerevisiae*, LA factor and ABC transporter genes exhibit varying degrees of redundancies. This yeast has two LA factors, both of which are thought to be components of ceramide synthase, the target site of fumonisins (Schorling et al., 2001). Each *S. cerevisiae* LA factor can compensate for the absence of the other: deletion of either gene does not affect ceramide synthase activity, but deletion of both genes markedly impairs activity. Even when both LA factor genes are deleted, their functions are partially compensated for by two ceramidases that have low levels of ceramide synthesis activity (Schorling et al., 2001). Since LA factors are required for sphingolipid biosynthesis and are found widely in eukaryotic organisms, it is plausible that *G. moniliformis* has genes encoding other LA factors and that these factors are able to compensate for *FUM17* and *FUM18*. *S. cerevisiae* and other fungi also produce multiple ABC transporters, some of which have at least partially redundant functions (Del Sorbo et al., 2000). Thus, other transport proteins may be able to compensate for *FUM19* when it is disrupted.

BLASTX analyses indicated that most of the other *FUM* genes encode enzymes with activities expected to be involved in biosynthesis of fumonisins based on the chemical structures of these toxins. Previously, the putative PKS encoded by *FUM1* (= *FUM5*) was predicted to catalyze the synthesis of a linear 18-carbon polyketide that forms C-3–C-20 of the fumonisin backbone (Proctor et al., 1999a,b). The initial description of *FUM1* did not include mention of the methyltransferase domain that lies between the dehydratase and enoyl reductase domains of the PKS. The presence of this domain suggests that the methyl groups at C-12 and C-16 of fumonisins are incorporated by the PKS during formation of the polyketide backbone. Thus, the hypothetical product of the PKS is a linear 18-carbon chain with a terminal carboxylic acid function and two methyl groups (Fig. 7A). The order of most subsequent steps in fumonisin biosynthesis is almost completely unknown, but precursor feeding studies and the structures of B fumonisins indicate that, once formed, the polyketide undergoes condensation with alanine, reduction of the terminal carbonyl to a hydroxyl, hydroxylation at four positions corresponding to C-5, C-10, C-14, and C-15 of the fumonisin backbone, and esterification of 6-carbon tricarboxylic acids to the C-14 and C-15 hydroxyls (Blackwell et al., 1994; Branham and Plattner, 1993; Caldas et al., 1998; Proctor et al., 1999a,b).

As reported in a previous study, the condensation of the fumonisin polyketide and alanine is likely to be catalyzed by the *FUM8* protein (Fig. 7B) in a manner analogous to the condensation of palmitic acid and serine by the enzyme serine palmitoyltransferase, which shares a high degree of amino acid sequence identity to the *FUM8* protein (Buede et al., 1991; Nagiec et al., 1994; Proctor et al., 1999a,b). Serine palmitoyltransferase and related aminotransferases catalyze the condensation of amino acids and CoA-activated acyl compounds (e.g., palmitoyl-CoA). Thus, the fumonisin polyketide is likely to be activated with CoA, prior to its condensation with alanine. One of the two putative fatty acyl-CoA synthetases, encoded by *FUM10* and *FUM16*, in the cluster could be responsible for this activation (Fig. 7B).

Reduction of the terminal carbonyl of the polyketide to a hydroxyl may be catalyzed by the *FUM13* protein, which exhibits similarity to short-chain dehydrogenases/reductases, many of which have carbonyl reductase activities. In sphingolipid metabolism, the reduction of the equivalent carbonyl occurs after the condensation of serine and palmitoyl-CoA (Merrill and Jones, 1990). If fumonisin and sphingolipid biosyntheses follow the same sequence of reactions, the fumonisin carbonyl would be reduced after the condensation of the polyketide and alanine (Fig. 7B).

Hydroxylation of the fumonisin backbone at C-5, C-10, C-14, and C-15 may be catalyzed by one or more of

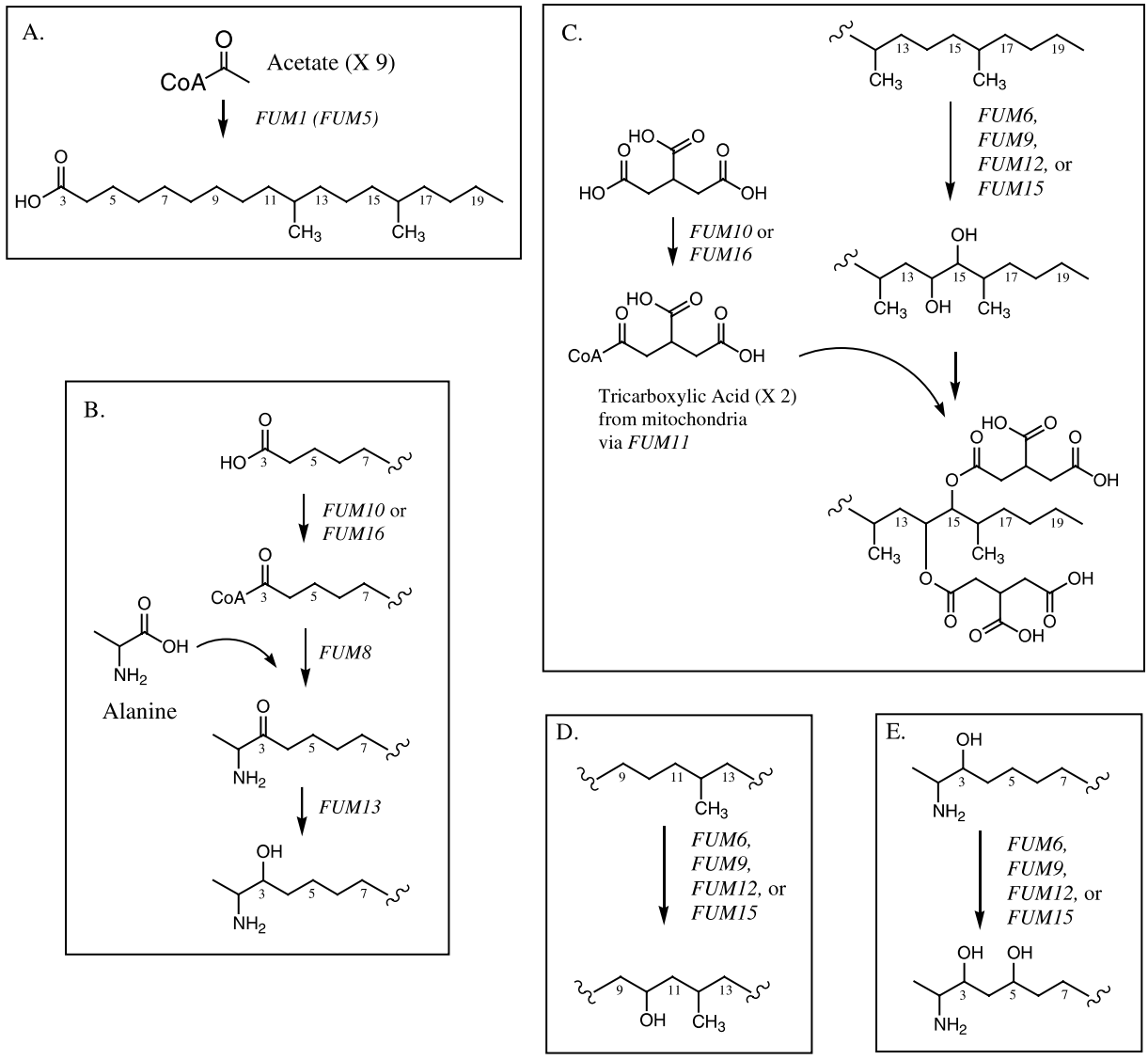

Fig. 7. Hypothetical functions of *FUM* gene products in fumonisin biosynthesis. (A) formation of the linear polyketide; (B) CoA activation, condensation with alanine, and carbonyl reduction of the polyketide; (C) CoA activation of tricarboxylic acids (TCAs), and hydroxylation and TCA esterification of the fumonisin backbone at C-14 and C-15; (D) hydroxylation of the backbone at C-10; and (E) hydroxylation of the backbone at C-5. The order of most reactions following the formation of the polyketide backbone is not known. Therefore, the order of reactions indicated by the lettering of schemes B–E may not reflect the order of reactions during fumonisin biosynthesis. The numbering of carbon atoms along the fumonisin backbone is the same before and after condensation with alanine. This numbering system is consistent with the text and Fig. 1.

the cytochrome P450 monooxygenases encoded by *FUM6*, *FUM12*, and *FUM15* and the putative oxoglutarate-dependent dioxygenase encoded by *FUM9* (Figs. 7C–E). Oxygenases of these types can catalyze a variety of biochemical reactions, but they are perhaps best known for their ability to catalyze hydroxylations (Precott, 2000; van den Brink et al., 1998). Both groups of enzyme use molecular oxygen as a source of oxygen in the formation of hydroxyl functions. The finding that the oxygen atoms at C-3, C-5, C-10, C-14, and C-15 of the fumonisin backbone are derived from molecular oxygen (Caldas et al., 1998) supports further a role for *FUM6*, *FUM9*, *FUM12*, and/or *FUM15* in the hydroxylation of the backbone. A previous study demonstrated that the *FUM6* protein is required for fumonisin production. However, its exact role could not be determined because no biosynthetic intermediates accumulated in *FUM6* disruption mutants (Seo et al., 2001). Genetic and biochemical analyses of natural variants of *G. moniliformis* indicate that the meiotically defined *Fum2* and *Fum3* loci confer the ability to hydroxylate the fumonisin backbone at C-10 and C-5, respectively (Desjardins et al., 1996). Complementation and disruption analyses are underway to determine whether any monooxygenase- or dioxygenase-encoding *FUM* genes correspond to the *Fum2* and *Fum3* loci.

Esterification of the 6-carbon tricarboxylic acids to the C-14 and C-15 hydroxyls on the fumonisin backbone may require at least two *FUM* genes in the cluster. The tricarboxylic acids are likely to be activated with CoA, prior to esterification. Thus, one of the fatty acyl-CoA synthetases encoded by *FUM10* and *FUM16* may catalyze this activation (Fig. 7C). In addition, the similarity of the *FUM11* protein to tricarboxylate transporters located in mitochondrial membrane suggests that its function may be to transport tricarboxylic acids from the mitochondria to make them available for fumonisin biosynthesis (Fig. 7C).

It is difficult to rationalize a role for *FUM14* in the biosynthesis of B fumonisins, because the structures of this series of fumonisins do not include amide functions. The predicted *FUM14* protein is similar to peptide synthetase condensation domains, which catalyze the formation of amides. However, the A-series fumonisins, which are produced by *G. moniliformis*, albeit at much lower levels than B fumonisins, have an amide function that results from the presence of an acetate moiety attached to the nitrogen atom at C-2 of the backbone (Bezuidenhout et al., 1988). The A fumonisins are structurally identical to B fumonisins in all other respects. Thus, a possible function for the *FUM14* protein is the condensation of an acetate unit with the C-2 nitrogen during A fumonisin synthesis.

The condensation domains to which the *FUM14* protein is similar are almost always located within multifunctional peptide synthetases that typically include at least two and as many as six other domains (e.g., adenylation, thiolation, and methyltransfer) in addition to the condensation domains (Marahiel et al., 1997). These peptide synthetases also have multiple copies of some or all domains. We are aware of only one other published example of a gene, the *Vibrio cholerae vibH* gene (Keating et al., 2000), that encodes a single condensation domain that is not part of a larger multidomain protein. Thus, the *FUM14* and *vibH* proteins are unusual in this respect.

Compared to most other fungal secondary metabolites for which gene clusters have been reported in the literature, fumonisins are simple molecules. As a result, we expect the biosynthetic pathway leading to their formation to be a relatively simple sequence of reactions. This is in contrast to more complicated pathways, leading to complex multicyclic compounds such as aflatoxins, gibberellins, penicillins, and trichothecenes. Despite the success of gene disruption experiments in demonstrating the function of other mycotoxin biosynthetic genes and despite the relative structural simplicity of fumonisins, gene disruption experiments have not demonstrated the exact role of any of the six *FUM* genes that have been disrupted. Nor have these experiments provided a clearer picture of the fumonisin biosynthetic pathway than was evident from prior biochemical studies. Disruption of three genes (*FUM17*, *FUM18*, and *FUM19*) in the current study did not affect fumonisin production or affected it only subtly and disruption of two other genes (*FUM6* and *FUM8*) in a previous study blocked production but did not lead to the accumulation of detectable intermediates (Seo et al., 2001). The failure of gene disruption to demonstrate the exact function of *FUM* genes may result from the structural similarities that fumonisins share with certain fatty acids and sphingolipid intermediates. These structural similarities may enable some fatty acid and sphingolipid metabolic enzymes to compensate for the absence of equivalent fumonisin biosynthetic enzymes. In addition, some fumonisin biosynthetic intermediates that accumulate in *FUM* gene mutants may be difficult to detect in an overwhelming pool of *G. moniliformis* fatty acids and sphingolipids with similar structures. Alternatively, some fumonisin intermediates may be diverted into lipid metabolism when fumonisin production is blocked. We are in the process of disrupting the remaining *FUM* genes to determine whether they function in fumonisin biosynthesis and in the hopes of identifying biosynthetic intermediates. In addition, we and other researchers are exploring alternative approaches, such as overexpression of *FUM* proteins, to determine *FUM* gene function and to elucidate further the fumonisin biosynthetic pathway.

Acknowledgments

We gratefully acknowledge Stephanie N. Folmar, Marcie L. Moore, and Deborah S. Shane for the technical assistance, Lawrence Tjarks for oligonucleotide synthesis and DNA sequence analysis, and Raymond Sylvester for preparation of figures.

References

Ahn, J.H., Cheng, Y.Q., Walton, J.D., 2002. An extended physical map of the *TOX2* locus of *Cochliobolus carbonum* required for biosynthesis of HC-toxin. Fungal Genet. Biol. 35, 31–38.

Altschul, S.F., Madden, T.L., Schaffer, A.A., Zhang, J., Zhang, Z., Millwer, W., Lipman, D.J., 1997. Gapped BLAST and PSI-BLAST: a new generation of protein database search programs. Nucleic Acids Res. 25, 3389–3402.

Bezuidenhout, S.C., Gelderblom, W.C.A., Gorst-Allman, C.P., Horak, R.M., Marasas, W.F.O., Spiteller, G., Bleggaar, R., 1988. Structure elucidation of the fumonisins, mycotoxins from *Fusarium moniliforme*. J. Chem. Soc., Chem. Commun. 1988, 743–745.

Blackwell, B.A., Miller, J.D., Savard, M.E., 1994. Production of carbon 14-labeled fumonisin in liquid culture. J. AOAC Int. 77, 506–511.

Brandwagt, B.F., Mesbah, L.A., Takken, F.L.W., Laurent, P.L., Kneppers, T.J.A., Hille, J., Nijkamp, H.J.J., 2000. A longevity assurance gene homolog of tomato mediates resistance to *Alternaria alternata* f. sp. *lycopersici* toxins and fumonisin B1. Proc. Natl. Acad. Sci. USA 97, 4961–4966.

Branham, B.E., Plattner, R.D., 1993. Alanine is a precursor in the biosynthesis of fumonisin B_1 by *Fusarium moniliforme*. Mycopathologia 124, 99–104.

Brown, D.W., McCormick, S.P., Alexander, N.J., Proctor, R.H., Desjardins, A.E., 2001. A genetic and biochemical approach to study trichothecene diversity in *Fusarium sporotrichioides* and *Fusarium graminearum*. Fungal Genet. Biol. 32, 121–133.

Brown, D.W., McCormick, S.P., Alexander, N.J., Proctor, R.H., Desjardins, A.E., 2002. Inactivation of a cytochrome P-450 is a determinant of trichothecene diversity in *Fusarium* species. Fungal Genet. Biol. 36, 215–223.

Buede, R., Rinker-Schaffer, C., Pinto, W.J., Lester, R.L., Dickson, R.C., 1991. Cloning and characterization of *LCB1*, a *Saccharomyces* gene required for biosynthesis of the long-chain base component of sphingolipids. J. Bacteriol. 173, 4325–4332.

Caldas, E.D., Sadilkova, K., Ward, B.L., Jones, A.D., Winter, C.K., Gilchrist, D.G., 1998. Biosynthetic studies of fumonisin B_1 and AAL toxins. J. Agric. Food. Chem. 46, 4734–4743.

Del Sorbo, G., Schoonbeek, H.-J., De Waard, M.A., 2000. Fungal transporters involved in efflux of natural toxic compounds and fungicides. Fungal Genet. Biol. 30, 1–15.

Desjardins, A.E., Plattner, R.D., Proctor, R.H., 1996. Linkage among genes responsible for fumonisin biosynthesis in *Gibberella fujikuroi* mating population A. Appl. Environ. Microbiol. 62, 2571–2576.

Guillas, I., Kirchman, P.A., Chuard, R., Pfefferli, M., Jiang, J.C., Jazwinski, S.M., Conzelmann, A., 2001. C26-CoA-dependent ceramide synthesis of *Saccharomyces cerevisiae* is operated by Lag1p and Lac1p. EMBO J. 20, 2655–2665.

Gurr, S.J., Unkles, S.E., Kinghorn, J.R., 1987. The structure and organization of nuclear genes of filamentous fungi. In: Kinghorn, J.R. (Ed.), Gene Structure in Eukaryotic Microbes. IRL Press, Oxford, pp. 93–139.

Hohn, T.M., Krishna, R., Proctor, R.H., 1999. Characterization of a transcriptional activator controlling trichothecene toxin biosynthesis. Fungal Genet. Biol. 26, 224–235.

Howard, P.C., Eppley, R.M., Stack, M.E., Warbritton, A., Voss, K.A., Lorentzen, R.J., Kovach, R.M., Bucci, T.J., 2001. Fumonisin B1 carcinogenicity in a two-year feeding study using F344 rats and B6C3F1 mice. Environ. Health Perspect. 109 (S2), 277–282.

Jörnvall, H., Persson, B., Krook, M., Atrian, S., Gonzalez-Duarte, R., Jeffery, J., Ghosh, D., 1995. Short-chain dehydrogenases/reductases (SDR). Biochemistry 34, 6003–6013.

Keating, T.A., Marshall, C.G., Walsh, C.T., 2000. Vibriobactin biosynthesis in *Vibrio cholerae*: VibH is an amide synthase homologous to nonribosomal peptide synthetase condensation domains. Biochemistry 39, 15513–15521.

Keller, N.P., Hohn, T.M., 1997. Metabolic pathway gene clusters in filamentous fungi. Fungal Genet. Biol. 21, 17–29.

Kennedy, J., Auclair, K., Kendrew, S.G., Park, C., Vederas, J.C., Hutchinson, C.R., 1999. Modulation of polyketide synthase activity by accessory proteins during lovastatin biosynthesis. Science 284, 1368–1372.

Keyser, Z., Vismer, H.F., Klaasen, J.A., Snijman, P.W., Marasas, W.F.O., 1999. The antifungal effect of fumonisin B1 on *Fusarium* and other fungal species. S. Afr. J. Sci. 95, 455–458.

Lacombe, E., Hawkins, S., Van Doorsselaere, J., Piquemal, J., Goffner, D., Poeydomenge, O., Boudet, A.M., Grima-Pettenati, J., 1997. Cinnamoyl CoA reductase, the first committed enzyme of the lignin branch biosynthetic pathway: cloning, expression and phylogenetic relationships. Plant J. 11, 429–441.

Laich, F., Fierro, F., Cardoza, R.E., Martin, J.F., 1999. Organization of the gene cluster for biosynthesis of penicillin in *Penicillium nalgiovense* and antibiotic production in cured dry sausages. Appl. Environ. Microbiol. 65, 1236–1240.

Leslie, J.F., Plattner, R.D., Desjardins, A.E., Klittich, C.J.R., 1992. Fumonisin B_1 production by strains from different mating populations of *Gibberella fujikuroi* (*Fusarium* section Liseola). Mycotoxicology 82, 341–345.

Marahiel, M.A., Stachelhaus, T., Mootz, H.D., 1997. Modular peptide synthetases involved in nonribosomal peptide synthesis. Chem. Rev. 97, 2651–2673.

Marasas, W.F.O., 2001. Discovery and occurrence of the fumonisins: a historical perspective. Environ. Health Perspect. 109 (S2), 239–243.

Merrill, A.H., Jones, D.D., 1990. An update of the enzymology and regulation of sphingomyelin metabolism. Biochim. Biophys. Acta 1044, 1–12.

Munkvold, G.P., Desjardins, A.E., 1997. Fumonisins in maize: can we reduce their occurrence? Plant Dis. 81, 556–565.

Nagiec, M.M., Baltisberger, J.A., Wells, G.B., Lester, R.L., 1994. The *LCB2* gene of *Saccharomyces* and the related *LCB1* gene encode subunits of serine palmitoyltransferase, the initial enzyme in sphingolipid synthesis. Proc. Natl. Acad. Sci. USA 91, 7899–7902.

Nelson, P.E., Desjardins, A.E., Plattner, R.D., 1993. Fumonisins, mycotoxins produced by *Fusarium* species: biology, chemistry, and significance. Annu. Rev. Phytopathol. 31, 233–252.

Plattner, R.D., Shackelford, D.D., 1992. Biosynthesis of labeled fumonisins in liquid cultures of *Fusarium moniliforme*. Mycopathologia 117, 17–22.

Plattner, R.D., Weisleder, D., Poling, S.M., 1996. Analytical determination of fumonisins and other metabolites produced by *Fusarium moniliforme* and related species on corn. In: Jackson, L.S., DeVries, J.W., Bullerman, L.B. (Eds.), Fumonisins in Food. Plenum Press, New York, pp. 57–64.

Precott, A.G., 2000. Two-oxoacid-dependent dioxygenases: inefficient enzymes or evolutionary driving force. In: Romeo, J.T., Ibrahim, R., Varin, L., De Luca, V. (Eds.), Evolution of Metabolic Pathways. Pergamon, Amsterdam, pp. 249–284.

Proctor, R.H., Desjardins, A.E., Plattner, R.D., 1999a. Biosynthetic and genetic relationships of B-series fumonisins produced by *Gibberella fujikuroi* mating population A. Nat. Toxins 7, 251–258.

Proctor, R.H., Desjardins, A.E., Plattner, R.D., Hohn, T.M., 1999b. A polyketide synthase gene required for biosynthesis of fumonisin mycotoxins in *Gibberella fujikuroi* mating population A. Fungal Genet. Biol. 27, 100–112.

Sambrook, J., Fritsch, E.F., Maniatis, T., 1989. Molecular Cloning: A Laboratory Manual. Cold Spring Harbor Laboratory Press, Plainview, New York.

Schorling, S., Vallee, B., Barz, W.P., Riezman, H., Oesterhelt, D., 2001. Lag1p and Lac1p are essential for the acyl-CoA-dependent ceramide synthase reaction in *Saccharomyces cerevisiae*. Mol. Biol. Cell 12, 3417–3427.

Seo, J.-A., Proctor, R.H., Plattner, R.D., 2001. Characterization of four clustered and coregulated genes associated with fumonisin biosynthesis in *Fusarium verticillioides*. Fungal Genet. Biol. 34, 155–165.

Shim, W.-B., Woloshuk, C.P., 2001. Regulation of fumonisin B1 biosynthesis and conidiation in *Fusarium verticillioides* by a cyclin-like (C-type) gene, FCC1. Appl. Environ. Microbiol. 67, 1607–1612.

Stachelhaus, T., Mootz, H.D., Bergendahl, V., Marahiel, M.A., 1998. Peptide bond formation in nonribosomal peptide biosynthesis: catalytic role of the condensation domain. J. Biol. Chem. 273, 22773–22781.

Sydenham, E.W., Shephard, B., Thiel, P., 1992. Liquid chromatographic determination of fumonisins B1, B2, and B3 in foods and feeds. J. AOAC Int. 75, 313–318.

Tudzynski, B., Holter, K., 1998. Gibberellin biosysnthetic pathway in *Gibberella fujikuroi*: evidence for a gene cluster. Fungal Genet. Biol. 25, 157–170.

Turgeon, B.G., Garber, R.C., Yoder, O.C., 1987. Development of a fungal transformation system based on selection of sequences with promoter activity. Mol. Cell. Biol. 7, 3297–3305.

van den Brink, H.M., van Gorcom, R.F.M., van den Hondel, C.A.M.J.J., Punt, P.J., 1998. Cytochrome P450 enzyme systems in fungi. Fungal Genet. Biol. 23, 1–17.

Voss, T., Schulte, J., Tudzynski, B., 2001. A new MFS-transporter gene next to the gibberellin biosynthesis gene cluster of *Gibberella fujikuroi* is not involved in gibberellin secretion. Curr. Genet. 39, 377–383.

Wang, E., Norred, W.P., Bacon, C.W., Riley, R.T., Merrill, A.H., 1991. Inhibition of sphingolipid biosynthesis by fumonisins: implications for diseases associated with *Fusarium moniliforme*. J. Biol. Chem. 266, 14486–14490.

Woloshuk, C.P., Foutz, K.R., Brewer, J.F., Bhatnagar, D., Cleveland, T.E., Payne, G.A., 1994. Molecular characterization of *aflR*, a regulatory locus for aflatoxin biosynthesis. Appl. Environ. Microbiol. 60, 2408–2414.

Young, C., McMillan, L., Telfer, E., Scott, B., 2001. Molecular cloning and genetic analysis of an indole-diterpene gene cluster from *Penicillium paxilli*. Mol. Microbiol. 39, 754–764.

Yun, S.H., Arie, T., Kaneko, I., Yoder, O.C., Turgeon, B.G., 2000. Molecular organization of mating type loci in heterothallic, homothallic, and asexual *Gibberella fusarium* species. Fungal Genet. Biol. 31, 7–20.